Cooperative Shielding in Many-Body Systems with Long-Range Interaction

Lea F. Santos
Department of Physics, Yeshiva University, New York, New York 10016, USA and ITAMP, Harvard-Smithsonian Center for Astrophysics, Cambridge, Massachusetts 02138, USA

Fausto Borgonovi and Giuseppe Luca Celardo
Dipartimento di Matematica e Fisica and ILAMP, Universitá Cattolica del Sacro Cuore, 25121 Brescia, Italy and Istituto Nazionale di Fisica Nucleare, sez. Pavia, 27100 Pavia, Italy

(Received 1 November 2015; revised manuscript received 26 February 2016; published 21 June 2016)

In recent experiments with ion traps, long-range interactions were associated with the exceptionally fast propagation of perturbation, while in some theoretical works they have also been related with the suppression of propagation. Here, we show that such apparently contradictory behavior is caused by a general property of long-range interacting systems, which we name cooperative shielding. It refers to shielded subspaces that emerge as the system size increases and inside of which the evolution is unaffected by long-range interactions for a long time. As a result, the dynamics strongly depends on the initial state: if it belongs to a shielded subspace, the spreading of perturbation satisfies the Lieb-Robinson bound and may even be suppressed, while for initial states with components in various subspaces, the propagation may be quasi-instantaneous. We establish an analogy between the shielding effect and the onset of quantum Zeno subspaces. The derived effective Zeno Hamiltonian successfully describes the short-ranged dynamics inside the subspaces up to a time scale that increases with system size. Cooperative shielding can be tested in current experiments with trapped ions.

DOI: 10.1103/PhysRevLett.116.250402

Introduction.—A better understanding of the nonequilibrium dynamics of many-body quantum systems is central to a wide range of fields, from atomic, molecular, and condensed matter physics to quantum information and cosmology. New insights into the subject have been obtained thanks to the remarkable level of controllability and isolation of experiments with optical lattices [1–7] and trapped ions [8,9]. Recently there has been a surge of interest in the dynamics of systems with long-range interactions, triggered by experiments with ion traps [8,9], where the range of interactions in one-dimensional (1D) spin models can be tuned with great accuracy. Other realistic systems that contain long-range interaction include cold atomic clouds [10], natural light-harvesting complexes [11–13], helium Rydberg atoms [14], and cold Rydberg gases [15]. Long-range interacting systems display features that are not often observed in other systems, such as broken ergodicity [16–19] and long-lasting out-of-equilibrium regimes [20].

According to the usual definition [21], in d dimension, an interaction decaying as $1/r^{\alpha}$ (where r is the distance between two bodies), is short range when $\alpha > d$ and is long range when $\alpha \leq d$. A major topic of investigation has been whether the propagation of excitations in systems with long-range interaction remains confined or not to an effective light cone [22–30], as defined by the Lieb-Robinson bound [31] and its generalizations ([30] and references therein). In the aforementioned experiments with trapped ions, it was observed that for short-range interaction, the propagation of perturbation is characterized by a constant maximal velocity, being bounded to an effective light cone. As α decreases, the propagation velocity increases and eventually diverges. For long-range interaction, $\alpha < 1$, the light-cone picture is no longer valid and the dynamics becomes nonlocal. However, examples of constraint dynamics in long-range interacting systems have also been reported, including logarithmic growth of entanglement [23], light-cone features [30], self-trapping [32], and slow decays at critical points [33].

Here, we show that these contradictory results are due to a general effect present in long-range interacting systems, which we name cooperative shielding. It corresponds to the onset of approximate superselection rules that cause a strong dependence of the dynamics on the initial state. Inside a superselection subspace, long-range interactions do not affect the system evolution (shielding) up to a time scale that grows with system size (cooperativity). The dynamics can then be described by an effective short-ranged Hamiltonian that either leads to a propagation within the Lieb-Robinson light cone or to localization. In contrast, for an initial state with components over several subspaces, the propagation of excitations is affected by long-range interactions and can be unbounded.

To explain how shielding can arise in a very trivial case, let us consider the total Hamiltonian $H = H_0 + V$, describing a many-body quantum system, where H_0 has one-body terms and possible short-range interactions, and V corresponds to some additional interactions. If $[H_0, V] = 0$ and V is highly degenerate in one of its eigensubspaces $\mathcal{V}$, so

that $V|V_k\rangle = v|V_k\rangle$ for all $|v_k\rangle \in \mathcal{V}$, the evolution of any initial state $|\psi_0\rangle$ belonging to such eigensubspace is simply given by: $|\psi(t)\rangle = e^{-ivt/\hbar}e^{-iH_0t/\hbar}|\psi_0\rangle$. Since the only effect of V is to induce a global phase, the dynamics is shielded from V and determined only by H_0. In contrast, if the initial state has large components in more than one eigensubspace of V, the dynamics will not be shielded from V. The question that we now pose is whether shielding is still possible when $[H_0, V] \neq 0$ and V is no longer degenerate. We show that the answer is positive when V involves only long-range interactions. The dynamics can remain shielded, but now for a finite time that increases with system size.

One can also draw a parallel between the picture above and the quantum Zeno effect (QZE). In the QZE, the dynamics of the system remains confined to subspaces tailored by the interaction with a measuring apparatus [34–38]. The stronger the interaction is, the better defined the subspaces become. Here, instead, the interaction strength is kept fixed, but due to its long-range-nature, invariant subspaces are generated. The dynamics, restricted to the invariant subspaces, is described by a short-ranged Zeno Hamiltonian up to a time scale that diverges with system size.

The model.—We consider a 1D spin-1/2 model with L sites and open boundary conditions described by the Hamiltonian,

$$\begin{aligned} H &= H_0 + V, \\ H_0 &= \sum_{n=1}^{L}(\mathcal{B} + h_n)\sigma_n^z + \sum_{n=1}^{L-1} J_z \sigma_n^z \sigma_{n+1}^z, \\ V &= \sum_{n<m} \frac{J}{|n-m|^\alpha}\sigma_n^x \sigma_m^x. \end{aligned} \tag{1}$$

Above, $\hbar = 1$ and $\sigma_n^{x,y,z}$ are the Pauli matrices on site n. The transverse field has a constant component $\mathcal{B}$ and a random part given by h_n, where $h_n \in [-W/2, W/2]$ are random numbers from a uniform distribution. The nearest-neighbor (NN) interaction in the z direction, of strength $J_z \geq 0$, may or not be present. J is the strength of the interaction in the x direction with α determining the range of the coupling. Unless specified otherwise, $J = 1$. The Hamiltonian with $W = 0$ and $J_z = 0$ describes the systems studied with ion traps [8,9]. In agreement with those experiments, where a limited range of system sizes is explored, V is not rescaled by L.

When $\alpha = 0$, H can be written in terms of the total x magnetization, $M_x = \sum_{n=1}^{L} \sigma_n^x/2$, as

$$H = \sum_{n=1}^{L}(\mathcal{B} + h_n)\sigma_n^z + \sum_{n=1}^{L-1} J_z \sigma_n^z \sigma_{n+1}^z + 2JM_x^2 - \frac{JL}{2}. \tag{2}$$

The spectrum of V for $\alpha = 0$ is divided into energy bands, each one associated with a value of the collective quantity M_x^2. Each band, with energy $E_b = 2J(L/2 - b)^2 - JL/2$, has states with b and $L - b$ excitations, where $b = 0, 1, \ldots, L/2$. For instance, $b = 1$ corresponds to states with one spin pointing up in the x direction in a background of down-spins and vice-versa. An energy band contains $2\binom{L}{b}$ degenerate states if $b < L/2$ and $\binom{L}{b}$ states when $b = L/2$. For $0 < \alpha < 1$, the subspaces of V are still separated in energy bands, but the states in each band are not all degenerate anymore. For $\alpha > 1$, the subspaces may overlap in energy.

Light cones.—In Refs. [8,9], the acceleration of the spreading of excitations and eventual surpassing of the Lieb-Robison bound achieved by decreasing α was verified for initial states corresponding to eigenstates of H_0, where each site had a spin either pointing up or down in the z direction. These initial states have components in all subspaces of V.

Motivated by the special role of the x direction in Eq. (2) and to show the main features of cooperative shielding, here we change the focus of attention to initial states with spins aligned along the x axis. They are the eigenstates of V and are denoted by $|V_k\rangle$. In Fig. 1, we show the evolution of the spin polarization, $\langle\sigma_n^x(t)\rangle$, for an initial state where all spins point up in x, except for the spin in the middle of the chain, which points down, so $M_x = L/2 - 1$ and $b = 1$.

In Fig. 1(a), where the interaction is short range ($\alpha = 3$), H_0 effectively couples states belonging to different subspaces of V. The effects of both H_0 and V lead to the evident light cone. This is no longer the case for long-range interaction ($\alpha < 1$), as exemplified in Figs. 1(b) and 1(c) for $\alpha = 0$ and 0.5. Their dynamics is frozen for a long time, which increases with the range of the interaction [compare the time scales in (b) and (c)] and with the system size (see the discussion below). The long-time localization of spin excitations in Figs. 1(b) and 1(c) is caused by both combined factors: the separated energy bands of V and

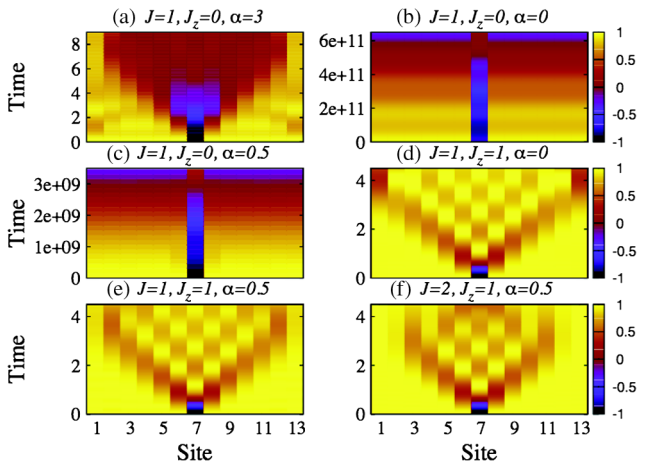

FIG. 1. Density plots for the evolution of $\langle\sigma_n^x(t)\rangle$; $L = 13$; $\mathcal{B}=1/2$; $W = 0$. Initial state: $\langle\sigma_7^x(0)\rangle = -1$ and $\langle\sigma_{n\neq7}^x(0)\rangle = +1$. A light cone typical of short-range interaction is seen in (a), as expected, but also in (d)–(f) where the evolution is shielded from the present long-range interaction. Freezing occurs for very long times in (b); it also happens in (c) where the bands of V are not degenerate.

the absence of direct coupling within the band (H_0 is not effective and $J_z = 0$). Notice that the energy bands for case (c) are no longer degenerate, yet localization persists for a long time.

Since the initial state is not an eigenstate of the total Hamiltonian, the spin excitation does eventually spread and the spins reverse their signs (see Figs. 1(b) and 1(c) at long times and discussion in [39]). This magnetic reversal can be explained in terms of macroscopic quantum tunneling [17].

While for $\alpha < 1$ in the presence of an external field the dynamics is frozen, the addition of NN interaction ($J_z \neq 0$) restores the propagation of perturbations [Figs. 1(d)–1(f)]. Despite the existence of long-range interactions, the evolution can be described by an effective short-ranged Hamiltonian, as we show below. This is the hallmark of the cooperative shielding effect discussed in this work, the suppression of propagation [Figs. 1(b) and 1(c)] being only a special case of it.

In Figs. 1(d)–1(f), a light cone typical of short-range interactions emerges: the dynamics is independent of system size and of the long-range coupling J. In Fig. 1(f), J is twice as large as in Figs. 1(d) and 1(e), but the results in the three panels are very similar, apart from border effects. The propagation of excitations depends only on J_z up to long times. This shielded evolution occurs for any $\alpha < 1$ (see more figures in [39]). In the case of $0 < \alpha < 1$, as in Figs. 1(e) and 1(f), the bands of V are no longer degenerate, so the various eigenstates of V that are excited within the band have different eigenenergies. One could then expect V to affect the evolution, yet the velocity of propagation remains independent of V for long times. This shows that the cause for shielding is not only the suppression of the transitions between different bands of V, but also the narrow distribution of the energies of V inside the band. The motion remains constrained to subspaces that are quasidegenerate with respect to V. The emergence of quasiconstants of motion is recurrent in long-range interacting systems [20].

Invariant subspaces and the Zeno effect.—Stimulated by the results of Fig. 1, we now analyze in more detail the effects of infinite-range interaction ($\alpha = 0$) and their dependence on system size. For a general treatment, we assume a random transverse field, so $\mathcal{B} = 0$ and $h_n \neq 0$. We take as the initial state $|\Psi(0)\rangle$ a random superposition of all states $|V_k^b\rangle$ that belong to the same fixed band b chosen for the analysis. We verified that the results for single states $|V_k^b\rangle$ picked at random from the same energy band are equivalent.

In Figs. 2(a) and 2(b), we compute the probability, $P_b(t)$, for the initial state to remain in its original energy band b,

$$P_b(t) = \sum_k |\langle V_k^b | e^{-iHt} | \Psi(0)\rangle|^2, \tag{3}$$

where the sum includes all the states of the selected energy band. The results are shown for $\langle P_b(t)\rangle$, where $\langle . \rangle$ indicates the average over random realizations of the transverse field

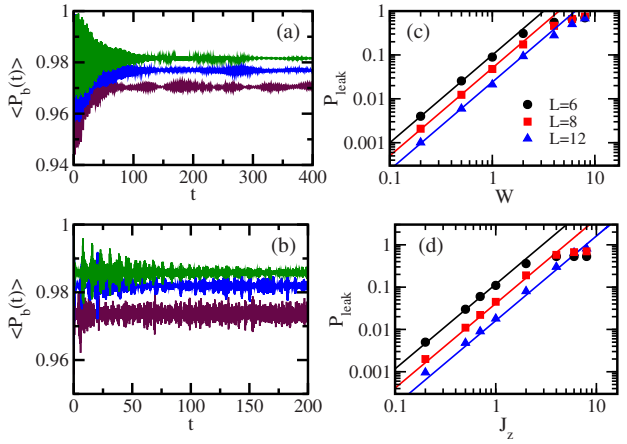

FIG. 2. Probability for the initial state to remain in [(a) and (b)] or leave [(c) and (d)] the band $b = 1$. The initial state is a random superposition of states $|V_k^b\rangle$. In (a) $J_z = 0$, $W = 2$ and in (b) $J_z = 1$, $W = 0$; $L = 10, 12, 14$ from bottom to top. In (c) P_{leak} vs W for $J_z = 0$ and in (d) P_{leak} vs J_z for $W = 0$. Symbols represent numerical results and full lines are analytical estimates [39] with an overall fitting multiplicative factor. In all panels: averages over 50 realizations, $\mathcal{B} = 0$, $\alpha = 0$.

and initial states. We show the case of $b = 1$, but similar results hold for other bands. It is evident that the probability to remain in the initial band increases with system size. This happens in the presence of a random transverse field [Fig. 2(a)] and also when NN interactions are added [Fig. 2(b)].

In Figs. 2(c) and 2(d), we plot the asymptotic values of the leakage probability, $P_{\text{leak}} = 1 - \lim_{t\to\infty}\langle P_b(t)\rangle$, as a function of the random field strength for $J_z = 0$ [Fig. 2(c)] and vs the NN coupling strength for $W = 0$ [Fig. 2(d)]. P_{leak} represents the probability for $|\Psi(0)\rangle$ to leak outside its original band. It decreases with L, showing that as the system size increases, the evolution of $|\Psi(0)\rangle$ remains more and more confined to a subspace of V for a longer time. Note that the distance between the bands nearby the initial one increases with L, but so does the number of states that are connected by H_0. The suppression of leakage takes into account this nontrivial interplay. A perturbative argument leads to $P_{\text{leak}} \propto (W/J)^2/L$ for $W \neq 0$ and $J_z = 0$, while $P_{\text{leak}} \propto (J_z/J)^2/L$ for NN interaction only [39]. Such scaling relations are consistent with our numerical data in Figs. 2(c) and 2(d).

The invariant subspaces generated by long-range interaction can be related to the QZE [34–38]. This term refers to the familiar freezing of the dynamics due to frequent measurements, but also to the onset of invariant Zeno subspaces that occurs in unitary dynamics due to strong interactions [36,38] and that has been studied experimentally [40]. The latter scenario is closer to our case and can be explained as follows. Consider the total Hamiltonian $H = H_s + gH_{\text{meas}}$, which one may interpret as a quantum system described by H_s that is continuously observed by an "apparatus" characterized by gH_{meas}. In the limit of strong

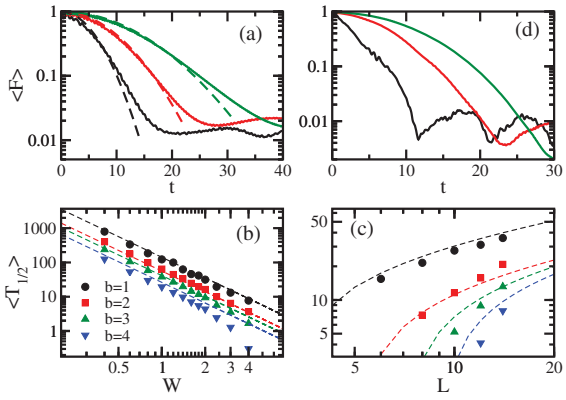

FIG. 3. Fidelity decay and time for it to reach the value $1/2$; initial states are random superpositions of $|V_k^b\rangle$. Upper panels: $F(t)$ for $b=3$ for $J_z=0$, $W=2$ (a) and for $W=0$, $J_z=1$ (d). From bottom to top: $L=10$, 12, 14. Numerical results: full lines. Gaussian decay: dashed lines. Lower panels have $J_z=0$ and give $T_{1/2}$ vs W for $L=12$ (b), and vs L for $W=2$ (c), for $|\Psi(0)\rangle$ from different bands. Numerical data: symbols. Analytical estimate $T_{1/2}=c_1/\delta E$ with c_1 being a fitting parameter: dashed lines. All panels: averages over 50 realizations, $\alpha=0$, $\mathcal{B}=0$.

coupling, $g\to\infty$, a superselection rule is induced that splits the Hilbert space into the eigensubspaces of $H_{\rm meas}$. Each one of these invariant quantum Zeno subspaces is specified by an eigenvalue v_k and is formed by the corresponding set of degenerate eigenstates of $H_{\rm meas}$. The dynamics becomes confined to these subspaces and dictated by the Zeno Hamiltonian $H_Z=\sum_k \Pi_k H_s \Pi_k + v_k \Pi_k$, where Π_k are the projectors onto the eigensubspaces of $H_{\rm meas}$ corresponding to the eigenvalues v_k.

For the system investigated here, we associate H_s with H_0 and $gH_{\rm meas}$ with V. The subspaces of V, with fixed numbers b of excitations, become invariant subspaces of the total Hamiltonian not only when $J\to\infty$ with $\mathcal{B}$, W, J_z fixed, which is the scenario of the QZE described above, but also in the large system size limit, $L\to\infty$, which is the main focus of this work.

When $J_z=0$, the Zeno Hamiltonian coincides with V, because H_0 does not directly couple states $|V_k^b\rangle$ that belong to the same eigensubspaces of V, so $\sum_k \Pi_k H_0 \Pi_k = 0$. This explains why the dynamics in Fig. 1(b) is frozen for very long times. On the other hand, in the case where $\mathcal{B}$, $W=0$ and $J_z\neq 0$, we can rewrite H_0 in terms of the $\sigma_n^{\pm_x}$ operators that flip the spins in the x direction. The projection of the NN part of the Hamiltonian on the eigensubspaces of V leaves only the term $\sigma_n^{+_x}\sigma_{n+1}^{-_x}+\sigma_n^{-_x}\sigma_{n+1}^{+_x}$, which leads to a Zeno Hamiltonian with an effective NN interaction that conserves the number of excitations inside each band b. This explains why in Fig. 1(d) a light cone typical of short-range interactions appears.

Fidelity decay.—To substantiate that the dynamics in the subspaces with fixed b becomes indeed controlled by the Zeno Hamiltonian as L increases, we analyze the fidelity between an initial state evolved under the total Hamiltonian H and the same state evolved under H_Z,

$$F(t)=|\langle\Psi(0)|e^{iH_Z t}e^{-iHt}|\Psi(0)\rangle|^2. \tag{4}$$

It is clear that if $H\to H_Z$ then $F(t)\to 1$. The results are shown in Fig. 3. Equivalently to Fig. 2, we fix $\mathcal{B}=0$ and deal with averages over disorder and initial states, which gives $\langle F(t)\rangle$. $|\Psi(0)\rangle$ is again a random superposition of all states $|V_k^b\rangle$ belonging to the same band b.

In Figs. 3(a) and 3(d) the fidelity is plotted vs time for different system sizes for the band with $b=3$. In panel (a), H_0 contains only the random fields, while in (d), H_0 contains only the NN interaction. In both cases the fidelity decay slows down as the system size increases, confirming that H_Z determines the dynamics for large L.

For the $J_z=0$ case of Fig. 3(a), since the projection of H_0 on the b subspace is 0, the fidelity coincides with the survival probability, $F(t)=|\langle\Psi(0)|\Psi(t)\rangle|^2$, which, counterintuitively, decays slower as the system size increases. This shows that the dynamics localizes as $L\to\infty$.$F(t)$ decays as a Gaussian [41–45]—see the dashed lines in Fig. 3(a).

In Figs. 3(b) and 3(c) we study how the time $T_{1/2}$ that it takes for the survival probability to reach the value $1/2$ depends on the disorder strength (b) and on system size (c). Figure 3(b) provides information associated with the usual QZE, where the quantum Zeno subspaces are induced by decreasing the strength of H_0. One sees that the dynamics slows down with the reduction of disorder as $\langle T_{1/2}\rangle\propto W^{-2}$. In Fig. 3(c), $\langle T_{1/2}\rangle$ grows with L, corroborating our claims that the fidelity increases and the excitations become more localized as the system size increases.

The estimation of the dependence of $T_{1/2}$ on the parameters of H goes as follows. Since the eigenstates of V in each invariant subspace are degenerate, the perturbation H_0 mixes them all. In this case, the energy uncertainty ω of the initial state can be approximated by the energy spread δE of each band induced by the perturbation. The fidelity decay can then be estimated as $T_{1/2}\simeq 1/\delta E$, where δE is computed from perturbation theory [39]. For large system sizes one has $T_{1/2}\propto J\sqrt{L}/W^2$. The analytical estimates for $T_{1/2}$ are shown with dashed curves in Figs. 3(b) and 3(c). The agreement is excellent.

We note that $T_{1/2}$ gives the time scale over which the shielding effect persists. In finite systems, shielding is effective for a finite time that can, however, be exceedingly long, as shown in Fig. 3.

Conclusions.—We revealed a generic effect of long-range interacting systems: cooperative shielding. It refers to invariant subspaces that emerge as the system size increases. Inside these subspaces, the dynamics occurs as if long-range interaction was absent, being dictated by effective short-ranged Hamiltonians. A parallel was established between these Hamiltonians and Zeno Hamiltonians.

The analysis and control of nonequilibrium dynamics can never be detached from the initial state considered. For exactly the same Hamiltonian with long-range interaction, an initial state with components in the various subspaces induced by that interaction leads to a nonlocal propagation of perturbation, as demonstrated experimentally with ion traps [8,9], while an initial state belonging to a single subspace is unaffected by the long-range interaction, as verified here. Cooperative shielding could also be tested by those experiments.

We acknowledge useful discussions with R. Bachelard, A. Biella, G. G. Giusteri, F. Izrailev, R. Kaiser, S. Ruffo, and R. Trasarti-Battistoni. This work was supported by the NSF Grant No. DMR-1147430.

[1] S. Trotzky, P. Cheinet, S. Fölling, M. Feld, U. Schnorrberger, A. M. Rey, A. Polkovnikov, E. A. Demler, M. D. Lukin, and I. Bloch, Science **319**, 295 (2008).
[2] S. Trotzky, Y.-A. Chen, A. Flesch, I. P. McCulloch, U. Schollwöck, J. Eisert, and I. Bloch, Nat. Phys. **8**, 325 (2012).
[3] M. Gring, M. Kuhnert, T. Langen, T. Kitagawa, B. Rauer, M. Schreitl, I. Mazets, D. A. Smith, E. Demler, and J. Schmiedmayer, Science **337**, 1318 (2012).
[4] T. Fukuhara, A. Kantian, M. Endres, M. Cheneau, P. Schausz, S. Hild, D. Bellem, U. Schollwöck, T. Giamarchi, C. Gross *et al.*, Nat. Phys. **9**, 235 (2013).
[5] K. R. A. Hazzard, B. Gadway, M. Foss-Feig, B. Yan, S. A. Moses, J. P. Covey, N. Y. Yao, M. D. Lukin, J. Ye, D. S. Jin *et al.*, Phys. Rev. Lett. **113**, 195302 (2014).
[6] T. Langen, R. Geiger, and J. Schmiedmayer, Annu. Rev. Condens. Matter Phys. **6**, 201 (2015).
[7] B. Bauer, T. Schweigler, T. Langen, and J. Schmiedmayer, arXiv:1504.04288.
[8] P. Jurcevic, B. P. Lanyon, P. Hauke, C. Hempel, P. Zoller, R. Blatt, and C. F. Roos, Nature (London) **511**, 202 (2014).
[9] P. Richerme, Z.-X. Gong, A. Lee, C. Senko, J. Smith, M. Foss-Feig, S. Michalakis, A. V. Gorshkov, and C. Monroe, Nature (London) **511**, 198 (2014).
[10] E. Akkermans, A. Gero, and R. Kaiser, Phys. Rev. Lett. **101**, 103602 (2008).
[11] J. Grad, G. Hernandez, and S. Mukamel, Phys. Rev. A **37**, 3835 (1988).
[12] G. L. Celardo, F. Borgonovi, M. Merkli, V. I. Tsifrinovich, and G. P. Berman, J. Phys. Chem. C **116**, 22105 (2012).
[13] G. L. Celardo, G. G. Giusteri, and F. Borgonovi, Phys. Rev. B **90**, 075113 (2014).
[14] Felix Jörder, K. Zimmermann, A. Rodriguez, and A. Buchleitner, Phys. Rev. Lett. **113**, 063004 (2014).
[15] M. M. Valado, C. Simonelli, M. D. Hoogerland, I. Lesanovsky, J. P. Garrahan, E. Arimondo, D. Ciampini, and O. Morsch, Phys. Rev. A **93**, 040701(R) (2016).
[16] D. Mukamel, S. Ruffo, and N. Schreiber, Phys. Rev. Lett. **95**, 240604 (2005).
[17] F. Borgonovi, G. L. Celardo, and G. P. Berman, Phys. Rev. B **72**, 224416 (2005).
[18] F. Borgonovi, G. L. Celardo, M. Maianti, and E. Pedersoli, J. Stat. Phys. **116**, 1435 (2004); F. Borgonovi, G. L. Celardo, A. Musesti, R. Trasarti-Battistoni, and P. Vachal, Phys. Rev. E **73**, 026116 (2006).
[19] G. L. Celardo, J. Barré, F. Borgonovi, and S. Ruffo, Phys. Rev. E **73**, 011108 (2006).
[20] R. Bachelard, C. Chandre, D. Fanelli, X. Leoncini, and S. Ruffo, Phys. Rev. Lett. **101**, 260603 (2008).
[21] E. A. T. Dauxois, S. Ruffo, and M. Wilkens, *Dynamics and Thermodynamics of Systems with Long-Range Interactions* (Springer, Berlin, 2002).
[22] M. Hastings and T. Koma, Commun. Math. Phys. **265**, 781 (2006).
[23] J. Schachenmayer, B. P. Lanyon, C. F. Roos, and A. J. Daley, Phys. Rev. X **3**, 031015 (2013).
[24] J. Eisert, M. van den Worm, S. R. Manmana, and M. Kastner, Phys. Rev. Lett. **111**, 260401 (2013).
[25] P. Hauke and L. Tagliacozzo, Phys. Rev. Lett. **111**, 207202 (2013).
[26] Z.-X. Gong, M. Foss-Feig, S. Michalakis, and A. V. Gorshkov, Phys. Rev. Lett. **113**, 030602 (2014).
[27] L. Mazza, D. Rossini, M. Endres, and R. Fazio, Phys. Rev. B **90**, 020301 (2014).
[28] D. Métivier, R. Bachelard, and M. Kastner, Phys. Rev. Lett. **112**, 210601 (2014).
[29] M. Foss-Feig, Z.-X. Gong, C. W. Clark, and A. V. Gorshkov, Phys. Rev. Lett. **114**, 157201 (2015).
[30] D.-M. Storch, M. van den Worm, and M. Kastner, New J. Phys. **17**, 063021 (2015).
[31] E. H. Lieb and D. W. Robinson, Commun. Math. Phys. **28**, 251 (1972).
[32] H. N. Nazareno and P. E. de Brito, Phys. Rev. B **60**, 4629 (1999).
[33] L. F. Santos and F. Pérez-Bernal, Phys. Rev. A **92**, 050101R (2015).
[34] A. Peres, Am. J. Phys. **48**, 931 (1980).
[35] P. Facchi and S. Pascazio, Fortschr. Phys. **49**, 941 (2001).
[36] P. Facchi and S. Pascazio, in *Progress in Optics*, edited by E. Wolf (Elsevier, Amsterdam, 2001), Vol. 42, pp. 147–217.
[37] P. Facchi and S. Pascazio, Phys. Rev. Lett. **89**, 080401 (2002).
[38] P. Facchi and S. Pascazio, in *Proceedings of the XXII Solvay Conference on Physics*, edited by I. Antoniou, V. A. Sadovnichy, and H. Walther (World Scientific, Singapore, 2003).
[39] See Supplemental Material at http://link.aps.org/supplemental/10.1103/PhysRevLett.116.250402 for further illustrations, discussions, and analytical estimates.
[40] J. M. Raimond, P. Facchi, B. Peaudecerf, S. Pascazio, C. Sayrin, I. Dotsenko, S. Gleyzes, M. Brune, and S. Haroche, Phys. Rev. A **86**, 032120 (2012).
[41] F. M. Izrailev and A. Castañeda-Mendoza, Phys. Lett. A **350**, 355 (2006).
[42] E. J. Torres-Herrera and L. F. Santos, Phys. Rev. A **89**, 043620 (2014).
[43] E. J. Torres-Herrera and L. F. Santos, Phys. Rev. E **89**, 062110 (2014).
[44] E. J. Torres-Herrera and L. F. Santos, Phys. Rev. A **90**, 033623 (2014).
[45] E. J. Torres-Herrera, M. Vyas, and L. F. Santos, New J. Phys. **16**, 063010 (2014).